Topology Comparison of Superconducting Generators for 10-MW Direct-Drive Wind Turbines: Cost of Energy Based

Liu, Dong; Polinder, Henk; Abrahamsen, Asger Bech; Ferreira, Jan Abraham

Published in:
I E E E Transactions on Applied Superconductivity

Link to article, DOI:
10.1109/TASC.2017.2668059

Publication date:
2017

Document Version
Peer reviewed version

Topology Comparison of Superconducting Generators for 10-MW Direct-Drive Wind Turbines: Cost of Energy Based

Dong Liu, *Student Member, IEEE,* Henk Polinder, *Senior Member, IEEE,*
Asger B. Abrahamsen, *Member, IEEE*, and Jan A. Ferreira, *Fellow, IEEE*

***Abstract*—This paper aims at finding feasible electromagnetic designs of superconducting synchronous generators (SCSGs) for a 10-MW direct-drive wind turbine. Since a lower levelized cost of energy (LCoE) increases the feasibility of SCSGs in this application, twelve generator topologies are compared regarding their LCoE in a simplified form of levelized equipment cost of energy (LCoE$_{eq}$). MgB$_2$ wires are employed in the field winding. Based on the current unit cost and critical current density capability of the MgB$_2$ wire at 20 K, the topologies with more iron have a much lower LCoE$_{eq}$ than the topologies with more non-magnetic cores. The fully iron-cored topology with salient poles has the lowest LCoE$_{eq}$. Then a scenario study shows that the difference of LCoE$_{eq}$ between the topologies will become much smaller when the unit cost of the MgB$_2$ wire drops to a quarter and the current density capability of the MgB$_2$ wire increases to 4 times. Then the topologies with more non-magnetic cores will become comparable to those with more iron. Aiming at a lower LCoE$_{eq}$ to increase the feasibility of SCSGs for large wind turbines, those topologies having the most iron in the core are the most promising for both now and the long term. If low weight is required, the topologies with more non-magnetic cores should be considered.**

***Index Terms*—Cost of energy, direct drive, MgB$_2$, superconducting generator, topology, wind turbine.**

I. Introduction

SUPERCONDUCTING synchronous generators (SCSGs) are drawing more attention for wind power conversion, because they can be lightweight and compact [1]-[3]. The INNWIND.EU project is now evaluating the feasibility of this technology for 10-20 MW direct-drive wind turbines [4].

Due to the high magnetic field production by superconducting (SC) coils, many possibilities exist for designing an SCSG. The SC coils are mostly applied in the DC field winding but can also be considered in the AC armature winding. A commonly applied approach is to use an SC field winding at a low temperature with a copper AC armature winding at an ambient temperature [5]-[8]. In such partially SCSGs, excessive AC losses in the SC armature winding can be avoided and the feasibility of SCSGs increases. The possible choices of wires for the field coils range from the low temperature superconductors (LTS) to the high temperature superconductors (HTS) with operation temperatures between 4-10 K and 20-40 K, respectively. The MgB$_2$ superconductor with an operation temperature between 10-20 K is an interesting alternative, since the cost of the wire is lower than that of the HTS and the cryogenic cooling system is simpler compared with the LTS.

For a partially SCSG design, many generator topologies can be considered from the perspective of electromagnetics. The topologies combine iron and non-magnetic cores in the rotor back core, rotor pole core, stator tooth and stator yoke. They differ in the magnetic reluctance of an electrical machine. The choice of topology could significantly change the cost and efficiency of an SCSG and consequently affect the cost of energy of a wind turbine employing this SCSG.

The cost of energy for an offshore wind turbine is often defined as the sum of the equipment (eq) cost and the Operation&Maintenance (O&M) cost normalized by the energy produced over the lifetime of the turbine. By also including the interest rates of the money flow during the lifetime then one can levelize the cost of energy to the start date of the turbine. This is termed Levelized Cost of Energy and can be written as

$$LCoE = LCoE_{eq} + LCoE_{O\&M} \tag{1}$$

This paper compares twelve superconducting generator topologies to identify the most feasible solution for a 10-MW direct drive wind turbine installed on a foundation for a water depth of 50 m. The comparison is done by formulating a simplified model only using the first term of Eq. (1): LCoE$_{eq}$ (levelized equipment cost of energy). This simplification assumes that the contribution of Operation&Maintenance can be considered to be identical to the level found for the INNWIND.EU reference turbine: $LCoE_{O\&M} \approx 24$ €/MWh [9]. The LCoE$_{eq}$ of the wind turbine and foundation is used as the criterion for this comparison, since a lower LCoE increases the feasibility of SCSGs in wind turbine applications. All the twelve topologies are optimized for their minimum LCoE$_{eq}$ before they are compared. Transportation and installation costs are not included in the LCoE model, since they are uncertain for such large turbines. Secondly they will most likely be similar for all direct-drive types of generators, since the boat rent and time usage are the cost drivers.

Three scenarios are studied to assess the effects of future improved properties of the employed MgB$_2$ superconductor on the comparison of the topologies. Besides the design objective

D. Liu, H. Polinder, and J. A. Ferreira are with the Department of Electrical Sustainable Energy, Delft University of Technology, NL-2628 CD Delft, Netherlands. E-mail: d.liu-1@tudelft.nl.

A. B. Abrahamsen is with DTU Wind Energy, Technical University of Denmark, DK-4000 Roskilde, Denmark.

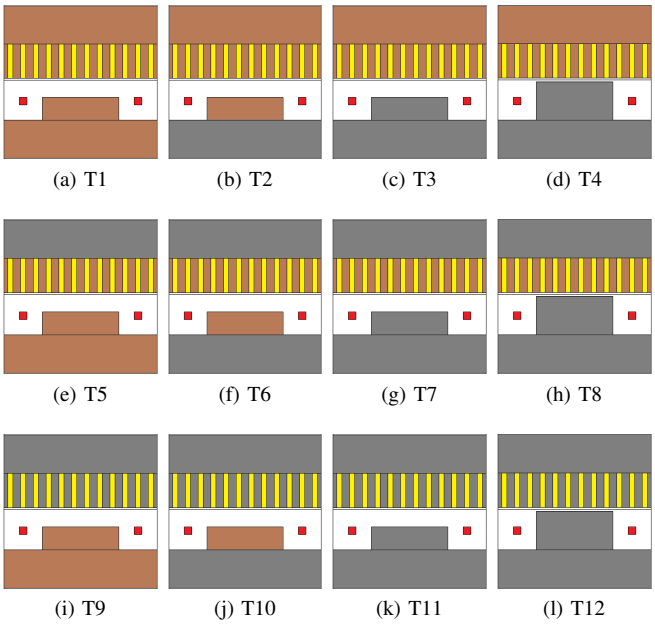

Fig. 1. Twelve topologies to be compared. Red: SC field winding. Yellow: copper armature winding. Brown: non-magnetic core. Gray: iron core.

of a low LCoE$_{eq}$, the comparison will also assess if the topologies will be sufficiently light compared to a reference low weight.

II. Generator to be Studied

A. Basic Characteristics

The partially SCSG for this study is required for a 10 MW direct-drive wind turbine installed on a fondation supporting a 50 m water depth defined by the INNWIND.EU project [4]. The rated speed is 9.6 rpm. The turbine rotor has a diameter of 178 m and its optimum tip speed ratio is 7.5. The maximum power coefficient of the turbine is 0.476. The air gap diameter of the SCSG is set to 6 m, because it is intended to be mounted in front of the turbine rotor blades [4]. The rated current density in the armature winding is 3 A/mm^2 and the armature slot filling factor is 0.6. The electrical loading limited below 75 kA/m (RMS) is to enable forced-air cooling on the armature winding [10]. The distance between the field winding and the stator bore is 50 mm including the cryostat wall, vacuum chamber and multilayer insulation. The employed MgB_2 wire is supplied by Columbus Superconductors [11].

B. Twelve Topologies

Combining iron and non-magnetic cores in the rotor back core, rotor pole core, stator tooth and stator yoke results in twelve applicable topologies (T1-T12) in total as shown in Fig. 1. In this list, nine topologies T1-T3, T5-T7, and T9-T11 have a large effective air gap length due to space allocated to the cryostat wall and thermal insulation. The other three topologies T4, T8 and T12 with salient iron poles at room temperatures have a significantly reduced effective air gap length. Because in these three topologies, the cryostat is made modular in the shape of racetrack and the iron pole can go as close to the stator as possible [12]-[15]. T4, T8 and T12 can be regarded as the extensions of T3, T7 and T11, respectively, from the topology point of view.

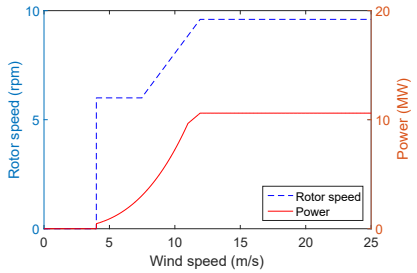

Fig. 2. Rotor speed and aerodynamic power of the reference wind turbine.

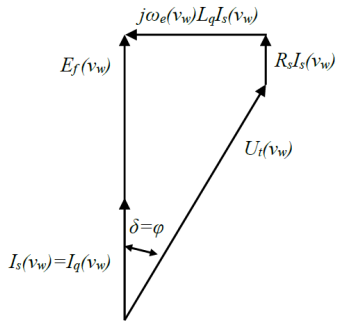

Fig. 3. Phasor diagram of the generator operating point, where v_w is wind speed. Voltages and currents are functions of wind speed.

C. Operation of Wind Turbine and Generator

The wind speed condition of the INNWIND.EU reference turbine is assumed to be Class Ia with a Weibull distribution of shape factor $k = 2$, scaling factor $A = 10.39$ [4]. The wind turbine operates following the rotational speed and power as a function of wind speed as shown in Fig. 2. The generator is operated under the phasor diagram given in Fig. 3, which is fully controlled by the power electronic converter. The phasor diagram is applied with the zero d-axis control with which the d-axis current of the generator remains zero and the torque is proportional to the q-axis current. The major advantage of this control strategy is relatively low copper losses in the armature winding. This phasor diagram of generator operation is a starting point and other operations can be studied in future.

The SC field winding of an SCSG is prone to AC losses when the field current is regulated in the way a conventional electrically excited synchronous generator is regulated. Thus, the field current must be changed sufficiently slowly and is changed only for regulations in hours or days. In this paper, we assume a constant field current of rated value throughout the full range of wind speed to neglect the field current regulation process at partial load.

III. Calculation of Levelized Cost of Energy

In this paper, the LCoE$_{eq}$ model of Eq. (1) is defined as

$$LCoE_{eq} = \frac{C_{act} + C_{other}}{a \cdot E_{AEP} \cdot T_{LT}} \tag{2}$$

TABLE I
ESTIMATION OF THE OTHER COSTS OF THE 10-MW INNWIND.EU WIND TURBINE

Parameter	Cost	Reference
Wind turbine (excl. gen. system)	7,500 k€	Cost model in [4]
Balance of plant	17,000 k€	Cost model in [4]
Power electronics C_{PE}	800 k€	Cost model in [4]
Cryogenic system C_{cryo}	600 k€	LTS SCSG in [16]
Generator supporting structures C_{str}	880 k€	LTS SCSG in [16]
Total C_{other}	26,780 k€	-

where C_{act} is the active material cost of the SCSG, C_{other} is the total cost of the other components of a wind turbine, E_{AEP} is the annual energy production, $a = 0.564$ is the annuity factor assuming a 5% interest, T_{LT} is the design life time of 25 years.

A. Costs

The choice of topologies changes C_{act} according to the materials usage. The other costs of the wind turbine C_{other} is assumed to be constant since C_{other} can hardly be changed by topology choice.

1) Active material cost: the active materials under consideration and their unit costs are

- MgB_2 wires for the field winding (1 or 4 €/m, depending on the used scenario),
- copper conductors for the armature winding (15 €/kg),
- ferromagnetic core material (3 €/kg), and
- non-magnetic core material (i.e. glass fiber G10) (15 €/kg).

2) Other costs: The cost of each component of the wind turbine and foundation are added up in C_{other} is given in Table I. The cryogenic system cost depends on a particular cryogenic design, and the cost estimation for supporting structures needs detailed mechanical analyses. Here these two costs are estimated based on a 13.2 MW LTS SCSG in [16].

The cost model from the INNWIND.EU project defines a reference 10-MW wind turbine and estimates the cost of each wind turbine component [4]. The total cost excluding C_{act} is roughly 27,000 k€ which is given to Eq. (2) as C_{other}. The costs of the turbine tower and the turbine foundation are assumed to be constant in Table I, because the wind loads are the main design drivers. This assumption neglects the influence of generator topologies on the costs of the supporting structures of the wind turbine. Therefore, the results of this paper, especially the size and mass of different topologies, need to be exported to structure designers to assess the structural costs for each generator topology. In this paper, the resulting active material masses of the topologies will be compared with a reference mass in Section VI to check if they reach low weight.

B. Power Losses

For calculating the AEP, all power losses and then the output power from the generator system should be calculated. The input power to the generator system P_{in} is the shaft power from the hub of a wind turbine. Assuming that mechanical losses, e.g. bearing and windage losses, are neglected, the input power is determined by the aerodynamic power from wind:

$$P_{in} = 0.5\rho_{air}C_p\pi r_{tr}^2 v_w^3 \tag{3}$$

where ρ_{air} is the mass density of air, C_p is the power coefficient of a wind turbine, r_{tr} is the turbine rotor radius, and v_w is the wind speed.

The total loss of the generator system P_{Loss} is calculated by

$$P_{Loss} = P_{Cu,joul} + P_{Cu,eddy} + P_{Fe,s} + P_{cryo} + P_{conv} \tag{4}$$

where $P_{Cu,joul}$ is the joule loss in the armature winding, $P_{Cu,eddy}$ is the copper eddy current loss in the armature winding which is modeled in [19], and $P_{Fe,s}$ is the iron loss in the armature iron core which is modeled in [20]. We assume that no losses exist in the field winding iron cores. The loss of the power electronic converter P_{conv} is modeled based on the current flowing in the power electronic switches [20].

The losses, both DC and AC losses, in the superconducting winding are negligibly small, according to [13]. Thus, these losses are not considered. The refrigeration for cooling the cryogenic environment for superconducting wires demands a power at an ambient temperature, which can also be considered as a power loss P_{cryo}. The cryogenic cooling power is estimated as 0.5% of the rated power of the SCSG. This estimation is based on the technical report by GE for an LTS SCSG design [21], which calculated the cryogenic cooling power at different wind speeds. This report shows that the cryogenic cooling power is constant with wind speed and it value is 22.5 kW. Here we assume a constant cryogenic cooling power of 50 kW at all wind speeds. This power value is more than doubled 22.5 kW to consider tolerances.

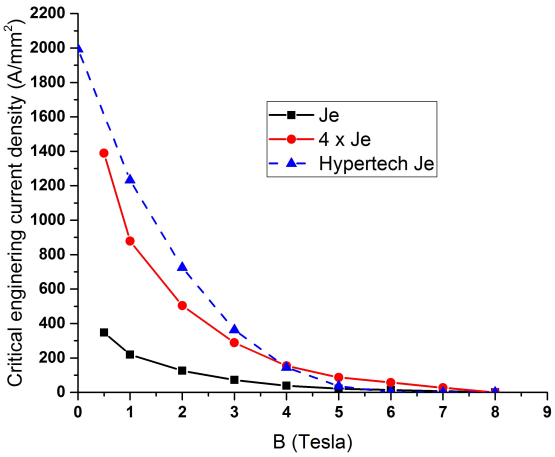

Fig. 4. Critical current density of MgB_2 wires with respect to magnetic flux density used for the scenario study. The curve Je is the critical current density of the MgB_2 supplied by Columbus Superconductors, reproduced from [17]. The curve 4 x Je increases the original curve of Je to 4 times. Hypertech Je is reproduced from [18] and this curve was a short-term prediction in [18]. The curve of 4 x Je fits well the predicted curve of Hypertech Je.

IV. OPTIMIZATION

The optimization objective function is $LCoE_{eq}$ given in Eq. (2). Only the equipment costs are considered. The opti-

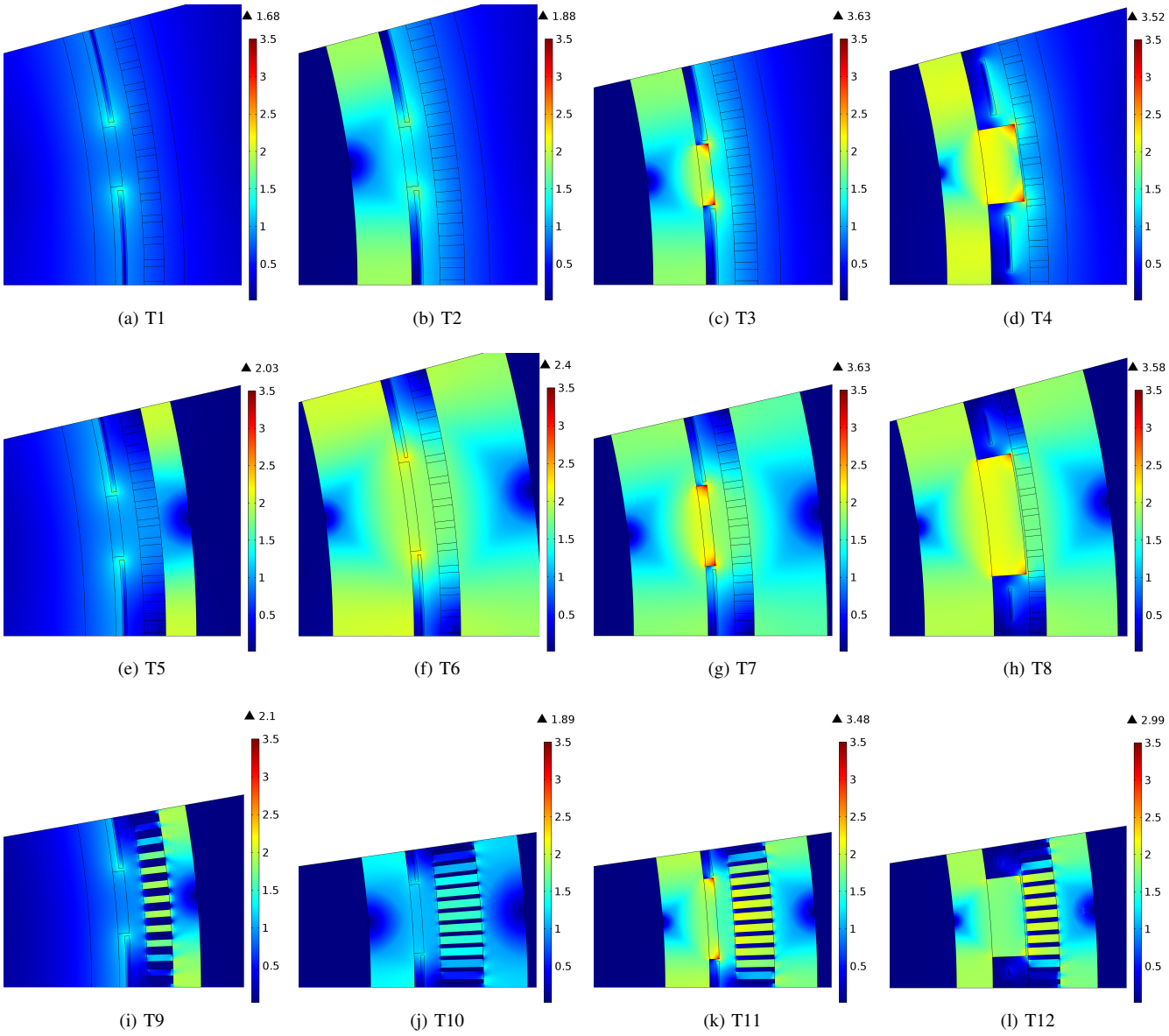

(a) T1 (b) T2 (c) T3 (d) T4

(e) T5 (f) T6 (g) T7 (h) T8

(i) T9 (j) T10 (k) T11 (l) T12

Fig. 5. One pole of the optimized twelve topologies in the original case (MgB_2 of 4 €/m and $1 \times J_e$) with the magnetic flux density distribution.

mization program combines finite element (FE) and analytical models. The FE models calculate magnetic fields and torques. The analytical models calculate power losses.

The optimization applies a genetic algorithm NSGA-II [22], so all the optimization variables can be integer and their step sizes of evolution can be manipulated. The number of individuals per generation is set to 50. Each individual is a set of the optimization variables values. The optimization process will proceed until all the individuals converge to the same minimum objective. Different initial individuals are used to check if the optimum is global. Details of the optimization method can be found in [23], [24].

V. Scenario Study

Besides the original case, three scenarios regarding the future development of the unit cost and the performance of MgB_2 wires are defined to investigate the influence on the topologies:

- Original: cost 4 €/m, current density capability J_e,
- Scenario 1: cost 1 €/m, current density capability J_e,
- Scenario 2: cost 4 €/m, current density capability $4J_e$,
- Scenario 3: cost 1 €/m, current density capability $4J_e$.

The original one is based on currently available commercial MgB_2 wires (supplied by Columbus Superconductors). Scenario 1 expects a lower unit cost (1/4) and Scenario 2 expects a higher current density capability (4 times). Scenario 1 is expected by the MgB_2 wire manufacturer when mass production is realized. Scenario 3 is considered as a long-term development goal. The current density capabilities used in the original case and in Scenario 2 and 3 are plotted in Fig. 4.

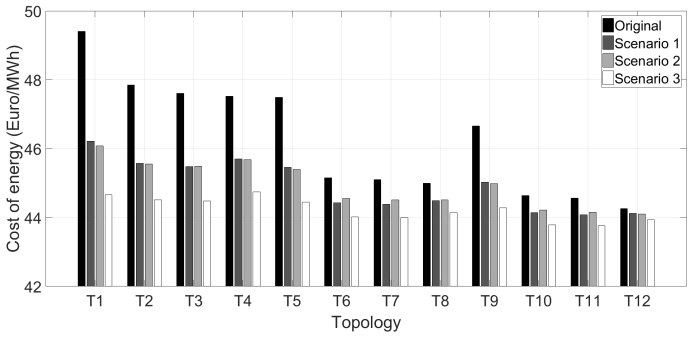

Fig. 6. Levelized cost of energy for equipment LCoE_{eq}.

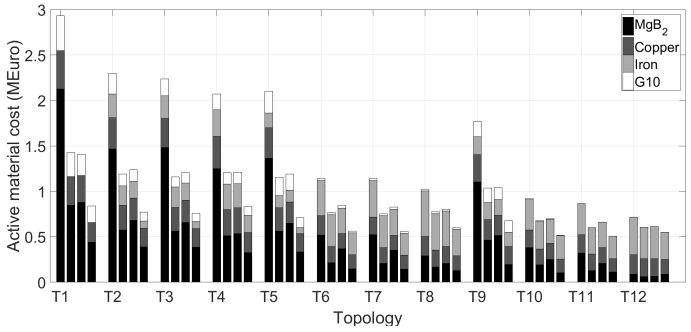

Fig. 7. Active material costs. Within a topology, the scenario changes from the left to the right.

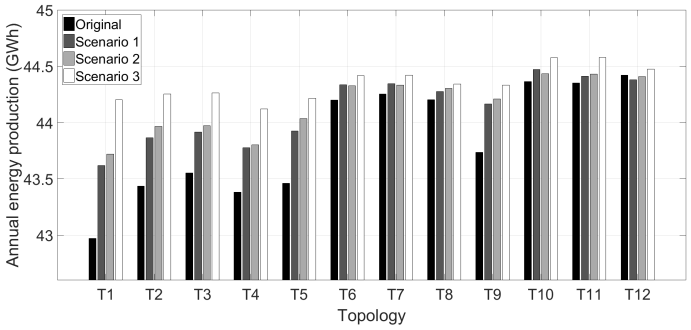

Fig. 8. Annual energy production.

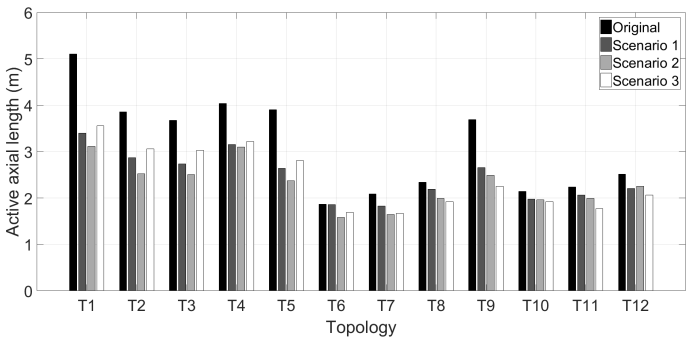

Fig. 9. Active generator length.

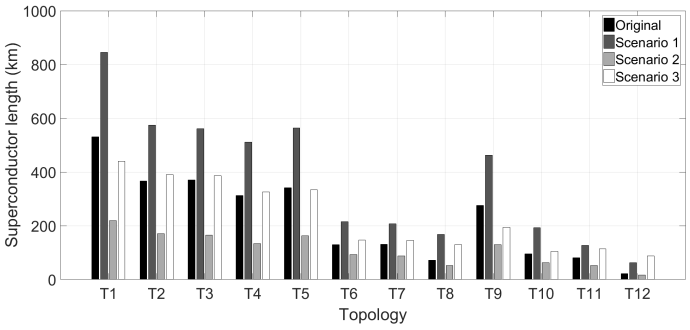

Fig. 10. Superconductor length.

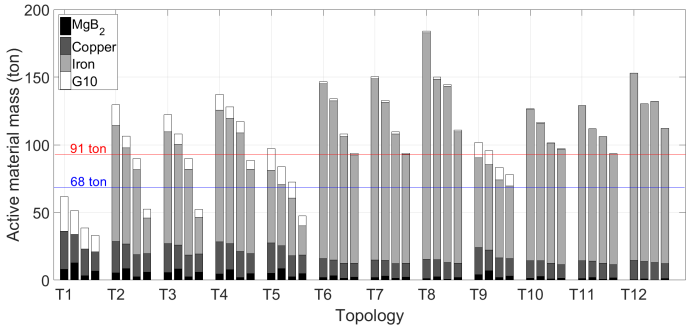

Fig. 11. Active material masses. Within a topology, the scenario changes from the left to the right.

VI. Comparison Results

The LCoE_{eq} and resulting generator characteristics, such as the active material cost, annual energy production (AEP), active generator length, superconductor length and active material mass, are obtained from the twelve optimized topologies in the original case and the three scenarios.

One pole of the optimized twelve topologies in the original case (MgB_2 of 4 €/m and J_e) is plotted in Fig. 5 with the magnetic flux density distribution. The topologies with iron stator teeth (T9-T12) have more pole pairs (18-24 pole pairs) than the other topologies (12-16 pole pairs). The optimized topologies from the three scenarios are omitted since the three scenarios do not change much the optimized geometry and the number of pole pairs. They mainly enlarge or reduce the cross-sectional area of the field coil since different amounts of SC wires are used due to the lower unit cost or the higher current density capability. Note that the topologies with salient poles (T4, T8 and T12) have smaller field coil pitches than other topologies since the modular cryostat occupies fixed space between two adjacent field coils.

The LCoE_{eq} is compared in Fig. 6. T12 has the lowest LCoE_{eq} (44.25 €/MWh) based on the current unit cost and critical characteristic of the MgB_2 wires. Change of scenarios does not make significant differences for T12. T1-T5 and T9 are much more expensive than the other topologies in the original case (e.g. 46.65 €/MWh for T9). However, they will greatly benefit from the lower unit cost and the higher current density capability of the MgB_2 wires (e.g. 44.32 €/MWh for T9 in Scenario 3). Changing to Scenario 1-3 effectively reduces the differences among the twelve topologies and Scenario 3 results in a much lower LCoE_{eq}. The topologies with more iron (T6-T8 and T10-T12) show advantages in the original cases while the topologies with more non-magnetic cores (T1-T5 and T9) will become competitive in Scenario 3.

In the three scenarios, T10 and T11 can become cheaper than T12 regarding the LCoE$_{eq}$. In addition, as shown in the results of Scenarios 1 and 2, either reducing the unit cost or increasing the capability of the MgB_2 wires can reach similar effects. Such beneficial effects from the original case to the scenarios can also be observed in the active material cost as compared in Fig. 7 and in the AEP as compared in Fig. 8.

The active generator length is compared in Fig. 9. T6 gives the shortest generator and the change of scenarios does not make much difference. In the three scenarios, the reduction of the generator length for the topologies with more non-magnetic cores (T1-T5 and T9) is more than for the others.

The superconductor length is compared in Fig. 10. In all the original case and the scenarios, applying the topologies with more iron can effectively shorten the length of superconducting wires. The advantage of short lengths is to facilitate the wire manufacturing. Moreover, as expected, cheaper MgB_2 wires results in more use thereof.

The active material mass is compared in Fig. 11. The topologies (T10-T12) that have a lower LCoE$_{eq}$ are heavier than the topologies that have a higher LCoE$_{eq}$ (T1-T5 and T9). A few reference generator masses can be introduced to define what a low weight is. One is the total mass of a 10-MW permanent magnet generator: $m_{PM} \approx 325$ ton [25]. One is the INNWIND.EU reference turbine drive train mass consisting of a medium speed gearbox and generator as well as the main shaft: $m_{innwind} \approx 227$ tons. [9]. The third is a reference total mass for a 10 MW SCSG design given in [26]. This reference mass indicates that a generator mass above 273 ton will significantly challenge the main bearing of the wind turbine rotor. The mass of 273 ton is about the average of m_{PM} and $m_{innwind}$. Therefore, this mass is used as a reference of low weight to evaluate the active material mass in Fig. 11. The active material mass could approximately be 1/3 to 1/4 of the generator mass (91 ton to 68 ton). This region of active material mass is also indicated in Fig. 11. In the original case, T1, T5 and T9 satisfy or almost satisfy 91 ton while only T1 satisfies 68 ton. None of the low-LCoE$_{eq}$ topologies (T10-T12) meet these low weights. The scenarios result in more lightweight topologies. For example, T4, T6, T7, T10-T12 satisfy 91 tons and T1-T3 and T5 satisfy 68 ton in Scenario 3. However, the low-LCoE$_{eq}$ topologies (T10-T12) are still far from 68 ton. The topologies that have a low LCoE$_{eq}$ may not be good options for low weight. If low weight is essential, the topologies with more non-magnetic cores that have higher LCoE$_{eq}$ should be considered.

VII. Conclusion

Twelve generator topologies for designing SCSGs have been compared regarding the LCoE$_{eq}$ for a 10-MW wind turbine. With the commercial MgB_2 wire in the field winding and based on the its current unit cost and current density capability, the topologies with more iron have a lower LCoE$_{eq}$ than the other topologies with more non-magnetic cores. The fully iron-cored topology with salient poles is most advantageous regarding the LCoE$_{eq}$ as well as the resulting active material cost, AEP and superconductor length.

As indicated in the scenario study, reducing the unit cost to a quarter or enhancing the current density capability to 4 times of the MgB_2 wire can effectively lower the LCoE$_{eq}$ for all the topologies, especially those with more non-magnetic cores. If both are combined as a long-term possibility, the difference of the LCoE$_{eq}$ between the topologies will become very small. Then the topologies with more non-magnetic cores will become comparable to those with more iron. Aiming at a lower LCoE, those topologies having the most iron in the core are most promising for both now and the long term. If low weight is required, the topologies with more non-magnetic cores should be taken into account.

Acknowledgment

This work is part of the INNWIND.EU project supported by the FP7 framework of EU, under grant agreement No. 308974.

References

[1] A. B. Abrahamsen, N. Mijatovic, E. Seiler, T. Zirngibl, C. Træholt, P. B. Nørgård, N. F. Pedersen, N. H. Andersen and J. Østergård, "Superconducting wind turbine generators," *Supercond. Sci. and Techno.*, vol. 23, pp. 034019, 2010.

[2] B. B. Jensen, N. Mijatovic, and A. B. Abrahamsen, "Development of superconducting wind turbine generators," *Journal of Renewable and Sustainable Energy*, vol. 5, pp. 023137, 2013.

[3] H. Polinder, J. A. Ferreira, B. B. Jensen, A. B. Abrahamsen, K. Atallah, and R. a. McMahon,"Trends in wind turbine generator systems," *IEEE J. Emerg. Sel. Top. Power Electron.*, vol. 1, pp. 174185, 2013.

[4] (2016, December) INNWIND.EU official website. [Online] Available: http://www.innwind.eu/

[5] Ronghai Qu, Yingzhen Liu and Jin Wang, "Review of superconducting generator topologies for direct-drive wind turbines," *IEEE Trans. on Appl. Supercond.*, vol. 23, pp. 5201108, June 2013.

[6] C. Lewis, and J. Muller, "A direct drive wind turbine HTS generator," *IEEE Power Engineering Society General Meeting*, pp. 1-8, 24-28 June 2007.

[7] G. Snitchler, B. Gamble, C. King, and P. Winn, "10 MW class superconductor wind turbine generators", *IEEE Trans. on Appl. Supercond.*, vol. 21, pp. 10891092, 2011.

[8] B. Maples, M. M. Hand, and W. D. Musial, "Comparative assessment of direct drive high temperature superconducting generators in multi-megawatt class wind turbines," Golden, CO: National Renewable Energy Laboratory, 2010.

[9] P. Chaviaropoulos and A. Natarajan, "Deliverable D1.2.2: Definition of Performance Indicators (PIs) and Target Values," Technical report, [Online] Available: http://www.innwind.eu/publications/deliverable-reports/.

[10] Juha Pyrhonen, Tapani Jokinen, and Valeria Hrabovcova, Design of Rotating Electrical Machines, New York: Wiley, 2009.

[11] (2016, December) Columbus Superconductors. [Online] Available: http://www.columbussuperconductors.com/.

[12] Y. Xu, N. Maki, L. Fellow, and M. Izumi,"Electrical design study of 10-MW salient-pole wind turbine HTS synchronous generators," *IEEE Trans. on Appl. Supercond.*, vol. 24, pp. 1-6, Dec. 2014.

[13] Dong Liu, H. Polinder, N. Magnusson, J. Schellevis, and A. B. Abrahamsen, "Ripple field AC losses in 10 MW wind turbine generators with a MgB_2 superconducting field winding," *IEEE Trans. on Appl. Supercond.*, vol. 26, no. 3, pp. 1-5, April 2016.

[14] H. Karmaker, M. Ho, D. Kulkarni, "Comparison between different design topologies for multi-megawatt direct drive wind generators using improved second generation high temperature superconductors," *IEEE Trans. on Appl. Supercond.*, vol. 25, pp. 1-5, June 2015.

[15] I. Marino et al., "Lightweight MgB_2 superconducting 10 MW wind generator," *Supercond. Sci. Technol.*, vol. 29, pp. 024005, Feb. 2016.

[16] Y. Liu, R. Qu, J. Wang, H. Fang, X. Zhang and H. Chen, "Influences of Generator Parameters on Fault Current and Torque in a Large-Scale Superconducting Wind Generator," *in IEEE Transactions on Applied Superconductivity*, vol. 25, no. 6, pp. 1-9, Dec. 2015.

[17] A. B. Abrahamsen, N. Magnusson, B. B. Jensen, D. Liu and H. Polinder "Design of an MgB_2 race track coil for a wind generator pole demonstration", *J. Phys.: Conf. Ser.*, vol. 507, pp. 032001, 2014.

[18] S. S. Kalsi,"Superconducting Wind Turbine Generator Employing MgB_2 Windings Both on Rotor and Stator," *IEEE Transactions on Applied Superconductivity,* vol. 24, no. 1, pp. 47-53, Feb. 2014.

[19] A. A. Arkadan, R. Vyas, J. G. Vaidya and M. J. Shah, "Effect of toothless stator design and core and stator conductors eddy current losses in permanent magnet generators," *IEEE Trans. on Energy Conversion*, vol. 7, pp. 231-237, March 1992.

[20] H. Polinder, F. F. Van Der Pijl, G. J. De Vilder, and P. J. Tavner, "Comparison of direct-drive and geared generator concepts for wind turbines," *IEEE Trans. Energy Convers.*, vol. 21, no. 3, pp. 725733, 2006.

[21] Fair, R. Superconductivity for Large Scale Wind Turbines, DOE report DE-EE0005143, 2012.

[22] K. Deb, A. Pratap, S. Agarwal, and T. Meyarivan, "A fast and elitist multiobjective genetic algorithm: NSGA-II", *IEEE Transactions on Evolutionary Computation*, vol.6, pp.182-197, April 2002.

[23] Dong Liu, H. Polinder, A. B. Abrahamsen and J. A. Ferreira, "Comparison of 10 MW superconducting generator topologies for direct-drive wind turbines," IEEE International Electric Machines & Drives Conference, Coeur D'Alene, USA, pp. 174-180, May 2015.

[24] D. Liu et al., "Comparison of superconducting generator topologies for a 10 MW wind turbine applications," International Journal of Applied Electromagnetics and Mechanics. (To be published soon) DOI: 10.3233/JAE-140161

[25] H. Polinder, D. Bang, R. P. J. O. M. van Rooij, A. S. McDonald and M. A. Mueller,"10 MW wind turbine direct-drive generator design with pitch or active speed stall control," 2007 IEEE International Electric Machines & Drives Conference, Antalya, 2007, pp. 1390-1395.

[26] A. B. Abrahamsen and A. Natarajan, "Variation of extreme and fatigue design loads on the main bearing of a front mounted direct drive system," *Journal of Physics: Conference Series,* vol. 765, no. 11, pp. 112006, 2016.